Electrodynamics of the Martian Dynamo Region

The M^4 Approach

Jérémy A. Riousset,[1] Carol S. Paty,[1] Robert J. Lillis,[2] Matthew O. Fillingim,[2] Scott L. England,[2] Paul G. Withers,[3] and John P. M. Hale[1]

[1]School of Earth and Atmospheric Sciences, Georgia Tech, Atlanta, GA, 30306, USA (riousset@gatech.edu)
[2]Space Sciences Lab, UC Berkeley, Berkeley, CA, 94720, USA
[3]Astronomy Department, Boston U, Boston, MA, 02215, USA

December 9th, 2013
AGU Suppl. Fall Meeting, San Francisco, CA

Abstract P12A-02
AGU

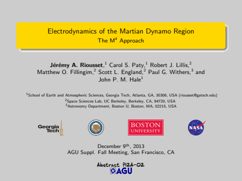

Keypoints:

- Mars is neither magnetized like Earth, Jupiter, Saturn, or Uranus, nor demagnetized like Venus: hence it is curious.
- Our work is a collaboration between intrumentalists (at SSL), and modelers (BU, GT, SSL).

30''

Outline

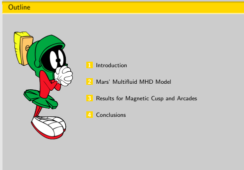

Keypoints:

- Mars is fascinating. *"He [Dave Brain] can't believe that someone is willing to pay him to think about Mars all day."* About Dave Brain as a Lecturer at Berkeley.
- Here my goal is to explain to you why we study Mars' ionosphere, how our group does it, and what our recent results are.

Mars' Dynamo Region (I)

- Definition: A **dynamo current** is generated by differential motions of positive and negative species.
- Mars' case:
  - ↳ positive ions → governed by collision with atmospheric wind-driven neutral particles (demagnetized)
  - ↳ electrons → governed by gyromotion (magnetized)

Magnetized ions Magnetized electrons	⇒ No dynamo current
Demagnetized ions Magnetized electrons	⇒ Ionospheric current
Demagnetized ions Demagnetized electrons	⇒ No differential current

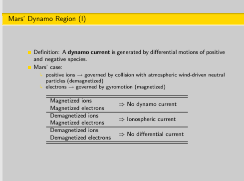

Keypoints:

- A dynamo current is generated by differential motions of positive and negative species. Between ∼100–200 km, ion motion is driven by collisions and electrons driven by the magnetic field.
- Above the dynamo regions, both electrons and ions are driven by the magnetic field (gyromotions), and below, there either absent (very low density) or guided by collisions.

- Estimates based on:
  - O_2^+: most abundant ion
  - CO_2: most abundant neutral
  - electron
- Altitudes:
  - H_L: lower boundary of the dynamo region
  - H_U: upper boundary of the dynamo region

$$\Omega_{O_2^+} = \nu_{O_2^+ - CO_2}(H_U) \quad \& \quad \Omega_e = \nu_{e-CO_2}(H_L)$$

$z \gtrsim H_U$	$\nu_{O_2^+ - CO_2} \ll \Omega_{O_2^+}$ $\nu_{e-CO_2} \ll \Omega_e$	Magnetized ions Magnetized electrons	⇒ No dynamo current
$H_L \lesssim z \lesssim H_U$	$\nu_{O_2^+ - CO_2} \gtrsim \Omega_{O_2^+}$ $\nu_{e-CO_2} \ll \Omega_e$	Demagnetized ions Magnetized electrons	⇒ Ionospheric current
$z \lesssim H_L$	$\nu_{O_2^+ - CO_2} \gtrsim \Omega_{O_2^+}$ $\nu_{e-CO_2} \gtrsim \Omega_e$	Demagnetized ions Demagnetized electrons	⇒ No differential current

2'00''

Mars' Dynamo Region (II)

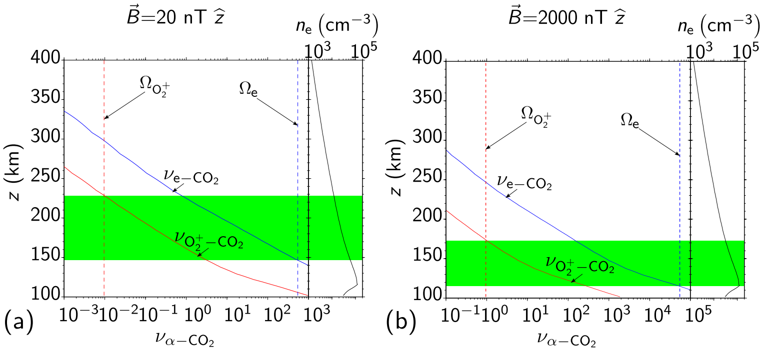

Figure: Expected locations of nighttime ionospheric currents (a) $\vec{B}$=20 nT $\hat{z}$ (typical); (b) $\vec{B}$=2000 nT $\hat{z}$ (near n_e peak).

Mars' Dynamo Region (II)

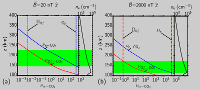

Figure: Expected locations of nighttime ionospheric currents (a) $\vec{B}$=20 nT $\hat{z}$ (typical); (b) $\vec{B}$=2000 nT $\hat{z}$ (near n_e peak).

Keypoints:

- In this graphical representation of the mechanisms described before, one can see that the altitude of the dynamo regions is directly dependent of the magnitude of the magnetic field.
- The collision frequency couples the charge carriers (ions and electrons) to the neutrals, while the gyrofrequency couples the charge carriers to the magnetic field. The green-shadowed region shows where ions and electrons are coupled to different processes.

3'00''

Objectives of the Study

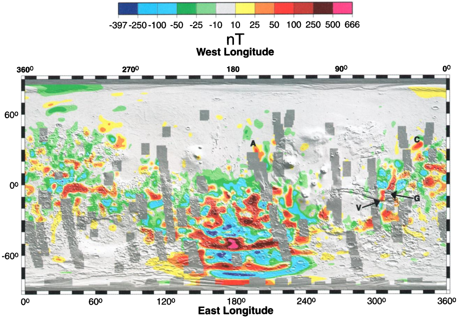

Figure: Radial magnetic field (B_r) computed at 200 km altitude in color, overlain on gray-shaded topographic gradient map of Mars (MOLA data). The dark grey bands show regions of inadequate data coverage [Purucker et al., 2000, Plate 1].

The M^4 approach [Riousset et al., 2013a]:

- **M**ars (CO_2, & O)
- **M**ultifluid (O_2^+, CO_2^+, O^+, & e)
- **M**agnetoHydroDynamic (MHD)
- **M**odel

Two case studies [Riousset et al., 2013b]:

- Cusp: case of the isolated buried magnetic dipole
- Arcades: striped magnetic topology

Objectives of the Study

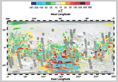

Figure: Radial magnetic field (B_r) computed at 200 km altitude in color, overlain on gray-shaded topographic gradient map of Mars (MOLA data). The dark grey bands show regions of inadequate data coverage [Purucker et al., 2000, Plate 1].

The M^4 approach [Riousset et al., 2013a]:

- **M**ars (CO_2, & O)
- **M**ultifluid (O_2^+, CO_2^+, O^+, & e)
- **M**agnetoHydroDynamic (MHD)
- **M**odel

Two case studies [Riousset et al., 2013b]:

- Cusp: case of the isolated buried magnetic dipole
- Arcades: striped magnetic topology

Keypoints:

- We are using a Multifluid, i.e., not particle approach to study the macroscopic dynamics of the atmospheric plasma, due to electromagnetic effects, and hydrodynamic (classic fluid mechanic effects) via MHD approach.
- Our work is based on observations of the planet's atmosphere and ionosphere (Viking) and magnetic fields (MGS/MagnetoMeter) to propose and explain of observable effects: Mars is losing its atmosphere.

3'30"

Initial Conditions

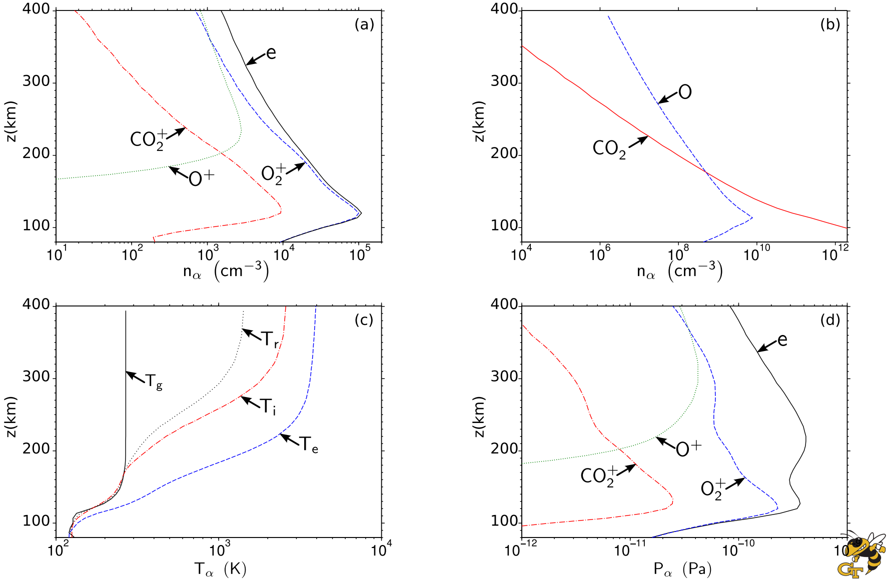

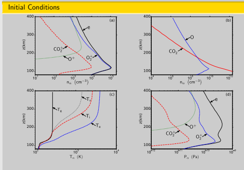

Keypoints:

- The only records of ion density profile we have come from Viking I and II landers in... 1976.
- We use a bit of ingeniosity to derive the fraction of each ion in the ionosphere and use the well-known electron density profiles to create our initial ionosphere. We top that with known temperature and neutral densities, complete it with the perfect gas law to create a full set of initial conditions.

Comments:

- Nighttime ionosphere (no photoionization)
- Non-uniform 3-D Cartesian grid:
  - -- 800 km×800 km×300 km
  - -- Horizontal resolution: 10.0–∼35 km
  - -- Vertical resolution: 4.0–∼22 km
- 2-step Runge-Kutta method [Balay et al., 1997; Pacheco, 1996; Press et al., 1992]

Comments (cont.):

- Initial conditions:
  - -- Horizontally uniform atmospheric/ionospheric profiles at t=0 s
  - -- $\vec{V}_{\mathrm{n}}$=100 m/s $\widehat{x}$
  - -- $\vec{V}_{\mathrm{i}}$=100 m/s $\widehat{y}$

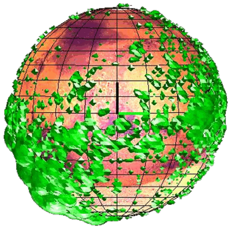

Figure: 100 nT surface levels of Mars' crustal fields using Purucker et al.'s [2000] magnetic field model [Brecht and Ledvina, 2010]. 4'30"

Multifluid Model Formulation

Based on Paty and Winglee [2006] for Ganymede published in [Riousset et al., 2013a]

- Conservation of matter (O_2^+, CO_2^+, & O^+)
- Plasma approximation (e)
- Equation of state (O_2^+, CO_2^+, O^+, & e)
- Conservation of momentum (O_2^+, CO_2^+, & O^+)
- Plasma current definition (e)
- Maxwell–Faraday equation ($\vec{B}$)
- Maxwell–Ampère equation ($\vec{J}$)
- Generalized Ohm's law ($\vec{E}$)

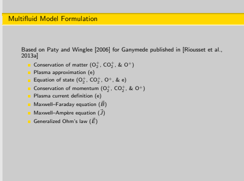

Keypoints:

- ''Fluid variables'' (densities, pressure, and velocities) are calculated using classic fluid equations (conservations of matter, momentum, and equation of state).
- ''Electromagnetic variables'' (magnetic field, current, and electric field) are calculated using Maxwell-Faraday and Maxwell-Ampère equations and the generalized Ohm's law.
- Our model is specific in that it does not define a conductivity coefficient but trully model its effects via the collisions (i-n, e-n, i-i, e-i). In the absence of such collisions, there is no dynamo region possible.
- No H^+, no IMF drapping field.

Comments:

- Fundamental equations
- Elastic ion–neutral collision
- Electron–neutral collisions (implemented)

$$
\begin{aligned}
\frac{\partial \vec{B}}{\partial t} &= -\nabla \times \vec{E} \\
\vec{J} &= \frac{\nabla \times \vec{B}}{\mu_0} \\
\vec{E} &= \frac{\vec{J} \times \vec{B}}{e n_e} - \sum_i \frac{n_i \vec{V}_i \times \vec{B}}{n_e} - \frac{\nabla P_e}{e n_e} + \frac{m_e}{e} \sum_n \nu_{n-e} \left(\vec{U}_n - \vec{V}_e \right) \\
\frac{\partial n_i}{\partial t} &= -\nabla \cdot \left(n_i \vec{V}_i \right) \\
n_e &= \sum_i n_i \\
\frac{\partial P_i}{\partial t} &= -\nabla \cdot \left(P_i \vec{V}_i \right) + (\gamma - 1) \vec{V}_i \cdot \nabla P_i \\
\frac{\partial P_e}{\partial t} &= -\nabla \cdot \left(P_e \vec{V}_e \right) + (\gamma - 1) \vec{V}_e \cdot \nabla P_e \\
\rho_i \frac{\partial \vec{V}_i}{\partial t} &= -\rho_i \left(\vec{V}_i \cdot \nabla \right) \vec{V}_i + q_i n_i \left(\vec{E} + \vec{V}_i \times \vec{B} \right) - \nabla P_i - \frac{\rho_i G M_M}{(R_M + r)^2} \hat{r} + \sum_n \rho_i \nu_{i-n} \left(\vec{U}_n - \vec{V}_i \right) \\
\vec{V}_e &= \sum_i \frac{n_i \vec{V}_i}{n_e} - \frac{\vec{J}}{e n_e}
\end{aligned}
$$

5'30''

Magnetic Field

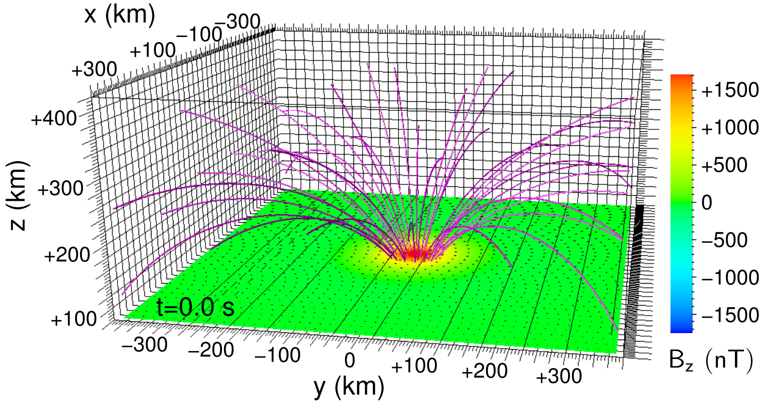

- Isolated dipole
- Vertical, upward, buried at –20 km
- Magnetic moment: $\vec{\mu}=10^{16}$ A·m^2 $\hat{z}$

- Analog to cusp (e.g., at (15°N;15°E) and (10°S;110°E))
- Building block for complex structure (loop, arcades)

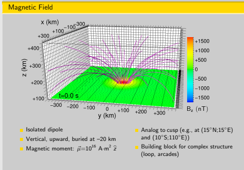

Keypoints:

- We simplify the problem into two fundamental cases: a magnetic cusp, and magnetic arcades. The first is both representative of local geometry, and building block of the second.
- In this first case, a single dipole is embedded at −20 km, and produces the cusp configuration, with reasonable magnetic field magnitudes.

Electric Field

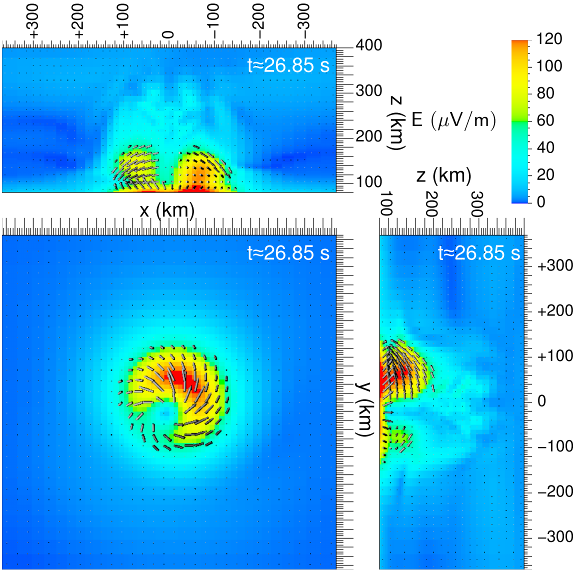

Generalized Ohm's law:

$$\vec{E} = \vec{E}_1 + \vec{E}_2 + \vec{E}_3 + \vec{E}_4$$

$$\vec{E}_1 = \frac{\vec{J} \times \vec{B}}{e n_\mathrm{e}}$$

$$\vec{E}_2 = -\sum_i \frac{n_i \vec{V}_i \times \vec{B}}{n_\mathrm{e}}$$

$$\vec{E}_3 = -\frac{\vec{\nabla} P_\mathrm{e}}{e n_\mathrm{e}}$$

$$\vec{E}_4 = \frac{m_\mathrm{e}}{e} \sum_{t=i,n} \nu_{t\mathrm{e}} \left(\vec{V}_t - \vec{V}_\mathrm{e} \right)$$

2013-12-13

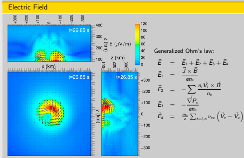

Keypoints:

- The effects of each component of the generalized Ohm's law can be visualized in this projection of the electric field in 3 planes (2 vertical planes and 1 horizontal at 112 km, in the dynamo region).
- The uniform neutral winds break the cylindrical symmetries creating the differences observed in the figure.

$\vec{E}_\alpha$	Direction of $\vec{E}_\alpha$
$\vec{E}_1 = \dfrac{\vec{J} \times \vec{B}}{e n_\mathrm{e}}$	$-\widehat{z}$ & outward directed from the cusp
$\vec{E}_2 = -\sum_i \dfrac{n_i \vec{V}_i \times \vec{B}}{n_\mathrm{e}}$	$+\widehat{y}$ & $\begin{cases} +\widehat{z} & \text{if } y \leq 0 \\ -\widehat{z} & \text{if } y \geq 0 \end{cases}$
$\vec{E}_3 = -\dfrac{\nabla P_\mathrm{e}}{e n_\mathrm{e}}$	$\begin{cases} -\widehat{z} & \text{if } z \leq 130 \text{ km} \\ +\widehat{z} & \text{if } 130 \leq z \leq 160 \text{ km} \end{cases}$
$\vec{E}_4 = \frac{m_\mathrm{e}}{e} \sum_{t=i,n} \nu_{te} \left(\vec{V}_t - \vec{V}_\mathrm{e} \right)$	$\begin{cases} \simeq \vec{0} \text{ away from the cusp} \\ \text{horizontal, CCW else} \end{cases}$

8'45''

Dynamo Current

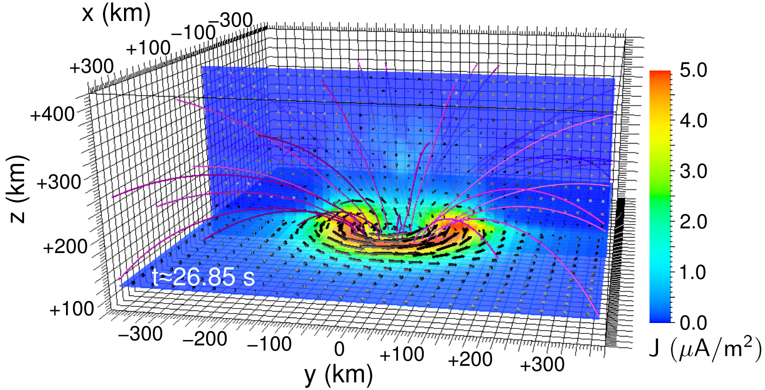

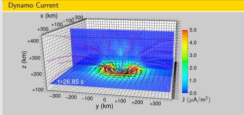

Keypoints:

- The ions are deviated into the neutral wind directions by collisions. Therefore, the torus-shaped current forms due to the $\vec{E}\times\vec{B}$-drift of electrons.
- One can verify that the direction of the current can also be retrieved from the right-hand rule: $\vec{J}=\dfrac{\nabla \times \vec{B}}{\mu_0}$

Comments:

- solid black arrows indicate the direction of the dynamo current
- solid magenta lines indicate the magnetic field lines

Magnetic Field

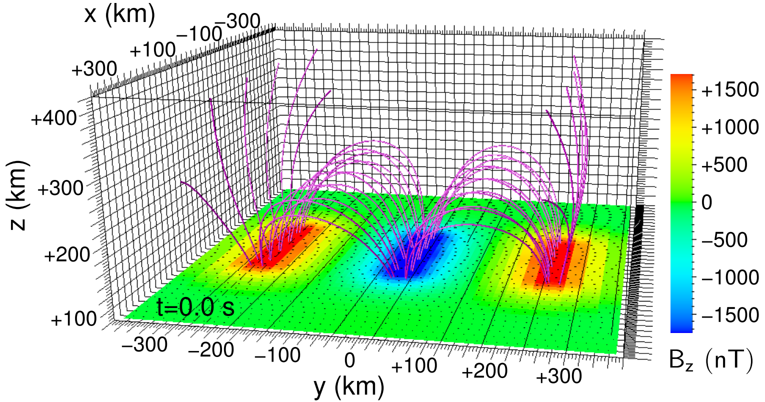

- 9 dipoles
- Vertical, upward and downward, buried at –20 km
- Magnetic moment: $\vec{\mu}=\pm 10^{16}$ A·m^2 $\hat{z}$

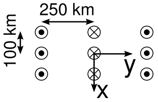

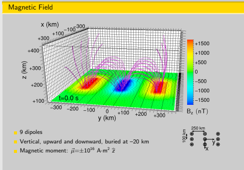

Keypoints:

- For illustrative/descriptive purposes, one can use as few as 9 dipoles to create reasonable magnetic arcades.
- We use three rows of dipoles evenly spaced, 100 km-apart. The central row is constituted of inverted diples, and flanked of two rows of upward dipoles just like the one we use to produce the previous example.
- Inverted dipoles act exactly as upward dipole except that they reverse the asymmetry in $\vec{E}$.

Dynamo Current

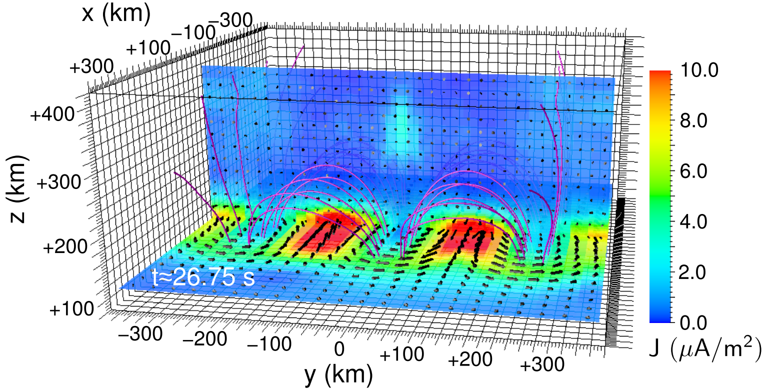

Dynamo Current

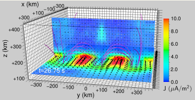

Keypoints:

- The organized pattern of the modeled dynamo current can be straightforwardly explained using the results magnetic dipoles, and the principle of superposition.
- There is a current developing above the regions of converging field lines, but not above the magnetic loops.

Results:

- The solid black arrows indicate the direction of the dynamo current.
- The colormap shows the amplitude of the current density with blue representing the lower values, and red the more intense currents.
- The solid magenta lines indicate the magnetic field lines.

11'00''

Principal Contributions

The principal results and contributions following from this work can be summarized as follows:

1. The dynamo current forms in a torus shape around the base of an isolated magnetic cusp due to the $\vec{E}\times\vec{B}$-drift of electrons;
2. The asymmetry in the horizontal component of the electric field is explained by the dependence of $\vec{E}$ on the collision-driven ion dynamics;
3. The organized pattern of the dynamo current produced by a striped magnetic field topology can be straightforwardly explained using the results from isolated vertically oriented, upward and downward magnetic dipoles, and the principle of superposition;
4. Strongly magnetized regions of Mars (e.g., Terra Sirenum) are likely to shield the local atmosphere and alter the motion of charged particles from the lower to the upper atmosphere.

Principal Contributions

The principal results and contributions following from this work can be summarized as follows:

- The dynamo current forms in a torus shape around the base of an isolated magnetic cusp due to the $\vec{E}\times\vec{B}$-drift of electrons;
- The asymmetry in the horizontal component of the electric field is explained by the dependence of $\vec{E}$ on the collision-driven ion dynamics;
- The organized pattern of the dynamo current produced by a striped magnetic field topology can be straightforwardly explained using the results from isolated vertically oriented, upward and downward magnetic dipoles, and the principle of superposition;
- Strongly magnetized regions of Mars (e.g., Terra Sirenum) are likely to shield the local atmosphere and alter the motion of charged particles from the lower to the upper atmosphere.

12'00''

Acknowledgments

THANK YOU FOR YOUR ATTENTION
QUESTIONS?

This work is available online at:
`http://www.jeremy.riousset.com/`

- Riousset et al. (2013), Three-dimensional multifluid modeling of atmospheric electrodynamics in Mars' dynamo region, *J. Geophys Res.*, 118(6), 3647–3659, doi: 10.1002/jgra.50328.
- Riousset et al. (2013), Electrodynamics of the Martian dynamo region near magnetic cusps and loops using the Martian Multifluid Magnetohydrodynamic Model (M^4), *Geophys. Res. Lett.*, doi: 10.1029/2013GL057589, *In review*.

This work was supported by the National Aeronautics and Space Administration under grant NNX10AM88G-MFRP to the Georgia Institute of Technology.

References

S. Balay, W. D. Gropp, L. C. McInnes, and B. F. Smith. Efficient management of parallelism in object oriented numerical software libraries. In E. Arge, A. M. Bruaset, and H. P. Langtangen, editors, *Modern Software Tools in Scientific Computing*, pages 163--202, Boston, MA, 1997. Birkhäuser Press. ISBN 978-1-4612-7368-4. doi: 10.1007/978-1-4612-1986-6_8.

S. H. Brecht and S. A. Ledvina. The loss of water from Mars: Numerical results and challenges. *Icarus*, 206(1): 164--173, 3 2010. ISSN 0019-1035. doi: 10.1016/j.icarus.2009.04.028.

P. S. Pacheco. *Parallel programming with MPI*. Morgan Kaufmann Publishers Inc., San Francisco, CA, 1996. ISBN 1-55860-339-5.

C. Paty and R. Winglee. The role of ion cyclotron motion at Ganymede: Magnetic field morphology and magnetospheric dynamics. *Geophys. Res. Lett.*, 33(10):L10106, 5 2006.

W. H. Press, B. P. Flannery, S. A. Teukolsky, and W. T. Vetterling. *Numerical Recipes in C: The Art of Scientific Computing*. Cambridge Univ. Press, Cambridge, UK; New York, NY, 2nd edition, 1992.

M. Purucker, D. Ravat, H. Frey, C. Voorhies, T. Sabaka, and M. Acuña. An altitude-normalized magnetic map of Mars and its interpretation. *Geophys. Res. Lett.*, 27:2449--2452, 8 2000. doi: 10.1029/2000GL000072.

J. A. Riousset, C. S. Paty, R. J. Lillis, M. O. Fillingim, S. L. England, P. G. Withers, and J. P. M. Hale. Three-dimensional multifluid modeling of atmospheric electrodynamics in Mars' dynamo region. *J. Geophys Res.*, 118 (6):3647--3659, 6 2013a. doi: 10.1002/jgra.50328.

J. A. Riousset, C. S. Paty, R. J. Lillis, M. O. Fillingim, S. L. England, P. G. Withers, and J. P. M. Hale. Electrodynamics of the Martian dynamo region near magnetic cusps and loops using the Martian Multifluid Magnetohydrodynamic Model (M^4). *Geophys. Res. Lett.*, 2013b. doi: 10.1029/2013GL057589. in review.